

NASA TECHNICAL NOTE



NASA TN D-6882

e. 1

NASA TN D-6882

LOAN COPY: RETURN TO
AFWL (DOUL)
KIRTLAND AFB, N. M.



AN INVESTIGATION OF PHOTSENSOR
APERTURE SHAPING IN FACSIMILE CAMERAS

*by Stephen J. Katzberg, Friedrich O. Huck,
and Stephen D. Wall*

*Langley Research Center
Hampton, Va. 23365*



0133740

1. Report No. NASA TN D-6882	2. Government Accession No.	3. Rec.	0133740	
4. Title and Subtitle AN INVESTIGATION OF PHOTORENSOR APERTURE SHAPING IN FACSIMILE CAMERAS		5. Report Date August 1972	6. Performing Organization Code	
		8. Performing Organization Report No. L-8424	10. Work Unit No. 502-03-52-04	
7. Author(s) Stephen J. Katzberg, Friedrich O. Huck, and Stephen D. Wall		11. Contract or Grant No.		
		13. Type of Report and Period Covered Technical Note		
9. Performing Organization Name and Address NASA Langley Research Center Hampton, Va. 23365		14. Sponsoring Agency Code		
		12. Sponsoring Agency Name and Address National Aeronautics and Space Administration Washington, D.C. 20546		
15. Supplementary Notes				
16. Abstract Optical-mechanical scanning techniques are generally employed in instruments specifically designed to spectrally or radiometrically characterize variations in scene brightness. The effect of aliasing, which can be caused by line-scan sampling, on the spatial detail of the reconstructed image has, therefore, been of little concern. Emphasis of some recent applications of optical-mechanical scanning techniques in facsimile cameras is, however, on the spatial characterization of the scene which, as is shown, can be severely degraded by aliasing. The characteristics of aliasing are analyzed to establish quantitative bounds, and photosensor aperture shaping and line-scan spacing are investigated as a means for reducing this degradation.				
17. Key Words (Suggested by Author(s)) Aliasing Aperture shaping Optical-mechanical scanner Facsimile camera		18. Distribution Statement Unclassified - Unlimited		
19. Security Classif. (of this report) Unclassified	20. Security Classif. (of this page) Unclassified	21. No. of Pages 15	22. Price* \$3.00	

AN INVESTIGATION OF PHOTSENSOR APERTURE SHAPING IN FACSIMILE CAMERAS

By Stephen J. Katzberg, Friedrich O. Huck,
and Stephen D. Wall
Langley Research Center

SUMMARY

Optical-mechanical scanning techniques are generally employed in instruments specifically designed to spectrally or radiometrically characterize variations in scene brightness. The effect of aliasing, which can be caused by line-scan sampling, on the spatial detail of the reconstructed image has, therefore, been of little concern. Emphasis of some recent applications of optical-mechanical scanning techniques in facsimile cameras is, however, on the spatial characterization of the scene which, as is shown, can be severely degraded by aliasing. The characteristics of aliasing are analyzed to establish quantitative bounds, and photosensor aperture shaping and line-scan spacing are investigated as a means for reducing this degradation.

INTRODUCTION

Translating variations in scene brightness into electrical video signals for spatial or spectral characterization requires optical-mechanical, diode array, or electron beam scanning techniques. The latter technique, generally using vidicon or image orthicon tubes, is most frequently employed when the principal purpose is to spatially characterize the scene. The effect of line-scan sampling on the reconstructed image has been studied for these devices in considerable detail during early television development (refs. 1 and 2). The optical-mechanical scanning technique, on the other hand, is most frequently employed when the principal purpose is to spectrally or radiometrically characterize the scene; and little attention has been paid to the effect of the line-scan process in such systems. However, in some recent applications of this technique, generally referred to as facsimile cameras on the USSR spacecraft Luna 9 (ref. 3), Luna 13 (ref. 4), and Lunokhod (ref. 5) and the U.S. spacecraft Viking lander (ref. 6), spatial characterization of the scene is most important.

Since scanning the scene is a spatial sampling process, the spatial frequency response of the optical system and the line-scan sampling interval must be carefully selected to avoid serious image degradation due to aliasing. Aliasing is a phenomenon

that occurs in sampling systems which have insufficiently bandlimited information or, equivalently, an insufficiently high sampling rate. In aliased data, high frequencies masquerade as low frequencies, giving rise to the name. Aliasing will almost always occur in facsimile camera systems which use only a single scan line per resolution element in order to minimize video data transmission requirements. Previous investigations of the line-scan sampling process (refs. 1 and 2) were concerned with modifying the intensity distribution of the scanning spot, either of electron beams in television or of light beams in film facsimile recorders, to reduce aliasing degradation. Direct application of these results to the optical-mechanical scanner would require shading the photosensor aperture with a variable transmission profile to obtain some desirable optical point spread function. Since facsimile cameras typically utilize apertures less than a millimeter across, realization of such a profile would be extremely difficult. However, the optical-mechanical scanner is free from some of the constraints imposed on electron or light beam scanning techniques and allows other approaches for reducing aliasing.

An analysis of the facsimile camera imaging process is presented, and those aspects which bear on aliasing are stressed. It is shown that common facsimile camera designs generate aliasing which can severely degrade the reconstructed image. The characteristics of aliasing are analyzed to establish quantitative bounds, and photosensor aperture shaping (rather than shading) is investigated as a means for reducing this degradation.

SYMBOLS

C	constant associated with aperture forms, radians
$f(\psi)$	aperture spatial extent, radians
F	spatial frequency passband of lens, cycles/radian
\mathcal{F}	Fourier transformation operator
$H(\chi, \psi)$	image plane intensity distribution, watts/radian ²
$I(\chi, \psi)$	photodetector output current, amperes
K, K_χ, K_ψ	spatial transform variables, cycles/radian
$L(\chi, \psi)$	lens point spread function
n	integer

$O(\chi, \psi)$	object plane intensity distribution, watts/radian ²
$P(\chi, \psi)$	photodetector sensitivity profile, amperes/watt
$p(\chi, \psi)$	realizable aperture primitive
Q	arbitrary integrated sensitivity function
$\sin \alpha$	optical numerical aperture
$\text{sinc}(n)$	sinc function, $(\sin \pi n)/\pi n$
$W(\psi)$	shaped aperture width, radians
Y	azimuth sampling interval, radians
δ	unit impulse function
λ	wavelength
χ	vertical angular coordinate, radians
ψ	azimuth angular coordinate, radians
Ψ	azimuth step interval, radians

III sampling (comb) function, $\sum_{n=-\infty}^{\infty} \delta(\psi-n)$

Subscripts:

A	aliasing function
s	scan angle
S	true signal
T	total signal

A caret over a symbol represents a Fourier transform variable.

ANALYSIS OF THE LINE-SCAN IMAGING PROCESS

In order to derive an analytical model of the facsimile camera, consider the system illustrated in figure 1. Radiation from the scene is captured by the scanning mirror and objective lens and projected onto a plane which contains the photosensor aperture. The photosensor converts the radiation falling on the aperture into an electrical signal. As the mirror rotates about a horizontal axis, the imaged scene moves past the aperture permitting the aperture to scan vertical strips. The camera is rotated slowly in azimuth so that the entire scene of interest is scanned. Spherical coordinates with an origin at the center of the objective lens are assumed as reference. Vertical and azimuthal coordinates are labeled χ and ψ , respectively, and angles through which the mirror has scanned the scene are labeled χ_s and ψ_s .

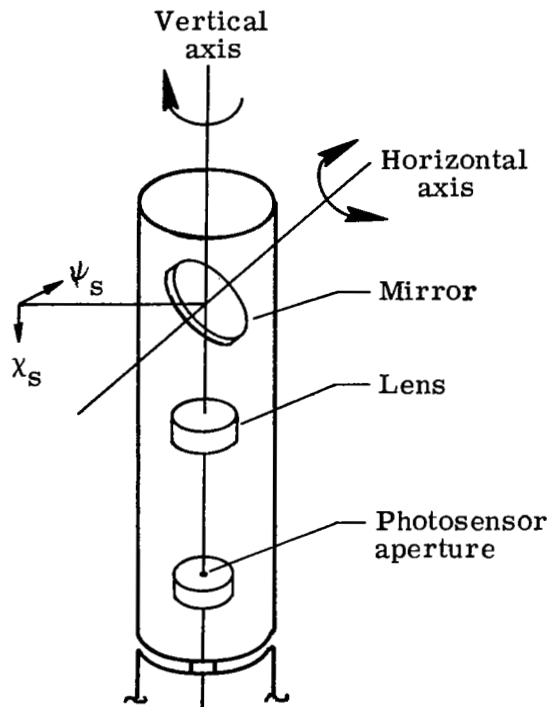


Figure 1.- Scanning geometry for facsimile camera.

The transfer of scene brightness $O(\chi, \psi)$ by the objective lens to the photosensor aperture plane may be expressed by the convolution

$$H(\chi, \psi) = \int_{-\infty}^{\infty} \int_{-\infty}^{\infty} O(\chi', \psi') L(\chi - \chi', \psi - \psi') d\chi' d\psi'$$

where $H(\chi, \psi)$ is the brightness distribution in the photosensor aperture plane, and $L(\chi, \psi)$ the lens point spread function. The effect of the scanning mirror is to shift the

angles χ and ψ by the scan angles χ_S and ψ_S (which are a function of time). Hence

$$H_S(\chi, \psi) = \int_{-\infty}^{\infty} \int_{-\infty}^{\infty} O(\chi' - \chi_S, \psi' - \psi_S) L(\chi - \chi', \psi - \psi') d\chi' d\psi' \quad (1)$$

The process by which the photodetector converts the radiant energy into an electrical signal may be expressed by

$$I(\chi_0, \psi_0) = \int_{-\infty}^{\infty} \int_{-\infty}^{\infty} H_S(\chi', \psi') P(\chi' - \chi_0, \psi' - \psi_0) d\chi' d\psi' \quad (2)$$

where $P(\chi, \psi)$ describes the angular extent of the aperture, as well as any transmission profile it may have, and $I(\chi, \psi)$ represents the detector output current if it were placed at coordinates χ_0, ψ_0 . Equations (1) and (2) can be collected to show the overall optical to electrical transformation:

$$I(\chi_0, \psi_0, \chi_S, \psi_S) = \int_{-\infty}^{\infty} \int_{-\infty}^{\infty} O(\chi_S - \chi', \psi_S - \psi') \int_{-\infty}^{\infty} \int_{-\infty}^{\infty} P(\chi'' - \chi_0, \psi'' - \psi_0) L(\chi'' - \chi', \psi'' - \psi') d\chi'' d\psi'' d\chi' d\psi' \quad (3)$$

Equation (3) may be conveniently rewritten using operator notation (and assuming $\chi_0 = \psi_0 = 0$) as

$$I(\chi_S, \psi_S) = O(\chi_S, \psi_S) * \left[P(\chi_S, \psi_S) * L(\chi_S, \psi_S) \right] \quad (4)$$

where $*$ represents the convolution operation.

Sampling of the scene is caused by the discrete azimuth steps between successive line scans. This may be expressed as (see ref. 7)

$$I_S(\chi_S, \psi_S) = \left\{ O(\chi_S, \psi_S) * \left[P(\chi_S, \psi_S) * L(\chi_S, \psi_S) \right] \right\} \frac{1}{Y} \text{III} \left(\frac{\psi_S}{Y} \right) \quad (5)$$

where Y represents the azimuth sampling interval. (For facsimile cameras used on planetary landers, this sampling interval is related to the angular azimuth stepping interval Ψ by $Y = \Psi \cos \bar{\chi}$ if $\bar{\chi}$ is measured from a plane normal to the optical axis of the objective lens.) Properties of the comb function III are discussed in references 7 and 8; but it may be pointed out that the comb function is essentially an infinite sum of delta functions whose spacing in this case is Y .

The spatial frequency characteristics of equation (5) can be found by taking its Fourier transform

$$\hat{I}_S(K_\chi, K_\psi) = \left[\hat{O}(K_\chi, K_\psi) \hat{P}(K_\chi, K_\psi) \hat{L}(K_\chi, K_\psi) \right] * \text{III}(YK_\psi) \quad (6)$$

where the carets represent the respective transform variables of the components in equation (5).

Two image degrading processes are described by the preceding equations; namely, blurring caused by the optical system response and aliasing caused by undersampling of the scene information which is passed by the optical system to the photosensor. The optical system response $\hat{L}(K_\chi, K_\psi) \hat{P}(K_\chi, K_\psi)$ of facsimile cameras is generally dominated by the photosensor aperture response $\hat{P}(K_\chi, K_\psi)$ for in- or near-focus imaging (ref. 9). The lens response will therefore be neglected here. But it is nevertheless useful to retain the fact that the lens limits the object spatial frequencies reaching the photosensor aperture. This spatial passband is designated by F . For a lens with a numerical aperture $\sin \alpha$, the region F is inside the circle $K^2 = K_\chi^2 + K_\psi^2 \leq \left(\frac{2 \sin \alpha}{\lambda}\right)^2$ where λ is the wavelength of the object radiation.

Aliasing and blurring are illustrated in figures 2 and 3 for a common facsimile camera design, using a circular photosensor aperture which forms an instantaneous field of view equal to the azimuth sampling interval Y . The one-dimensional frequency response of the imaging process along the (azimuth) ψ -direction, shown in figure 2, depicts blurring

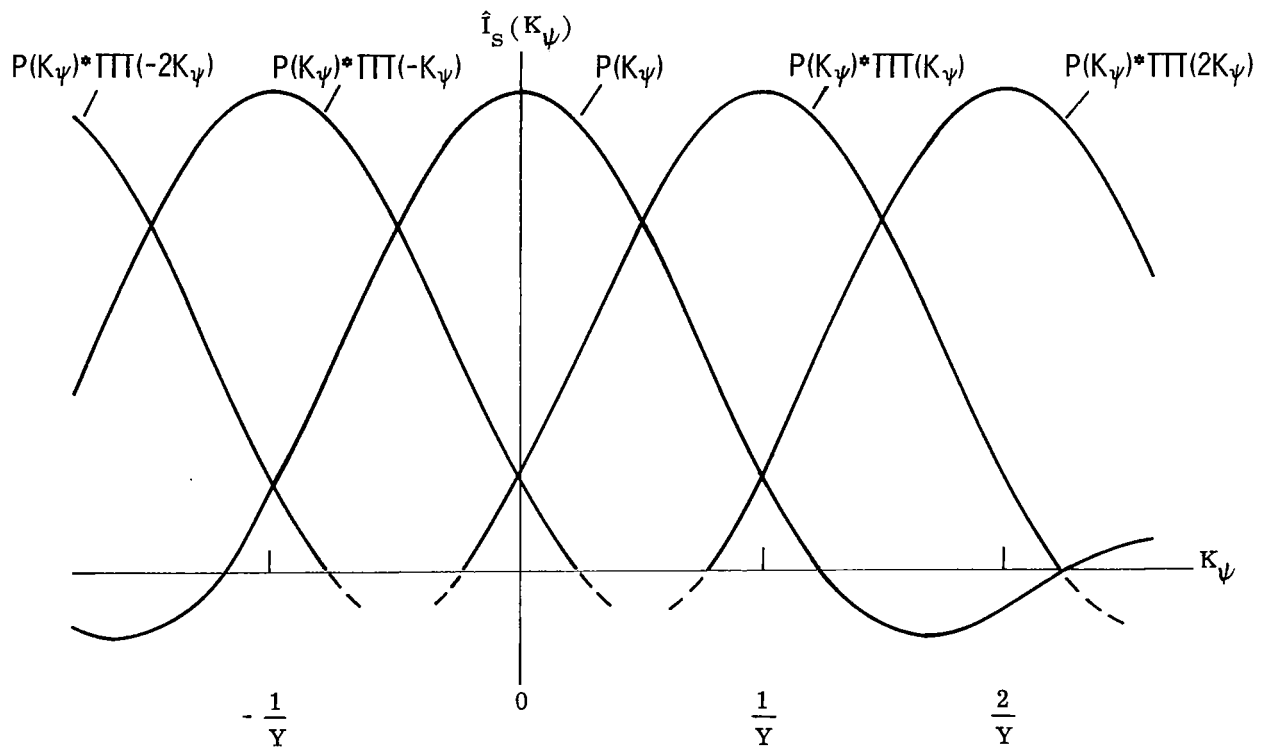


Figure 2.- Schematic representation of the frequency response normal to the line-scan direction of facsimile cameras in which the line-scan spacing is equal to the instantaneous field of view formed by a circular photosensor aperture.



(a) Targets.



(b) Images.

Figure 3.- Illustration of aliasing and blurring in facsimile camera images. The line-scan spacing is equal to the instantaneous field of view formed by a circular photo-sensor aperture.

by the decrease in frequency response with increasing spatial frequency K_ψ and aliasing by the overlap of the sidebands generated by sampling. Figure 3 shows experimental results. The decrease in contrast, best observed along the (line scan) χ -direction, is caused by blurring. The extraneous patterns along the (azimuth) ψ -direction are caused by aliasing. In general, scene information would be random rather than periodic, and the aliased signal would then be generally indistinguishable from the scene.

A MEASURE OF ALIASING

In order to properly consider the minimization of aliasing, an analytical measure must be set up which can then be used to compare aliased current with signal current. This may be done by dividing the total signal in a selected passband into two components, one resulting just from the pinhole modified scene information and the other resulting from the aliased bands:

$$I_T = I_S + I_A \quad (7)$$

where

$$I_S(\chi, \psi) = \iint_{\mathbf{F}} \hat{O}(K_\chi, K_\psi) \hat{P}(K_\chi, K_\psi) e^{2\pi i(K_\chi \chi + K_\psi \psi)} dK_\chi dK_\psi \quad (8)$$

and

$$I_A(\chi, \psi) = \iint_F \sum_{\substack{n \neq 0 \\ n=-\infty \\ n=\infty}}^{\infty} \hat{O}\left(K_\psi - \frac{n}{Y}, K_\chi\right) \hat{P}\left(K_\psi - \frac{n}{Y}, K_\chi\right) e^{2\pi i (K_\chi \chi + K_\psi \psi)} dK_\chi dK_\psi \quad (9)$$

Both equations (8) and (9) neglect the small degradation due to the objective lens, as was discussed previously. Equation (9) contains all sidebands which extend into the passband from the sampling sidebands. Taking the absolute magnitude gives

$$|I_A| \leq \iint_F \sum_{|n| \leq 2KY} \left| \hat{O}\left(K_\psi - \frac{n}{Y}, K_\chi\right) \hat{P}\left(K_\psi - \frac{n}{Y}, K_\chi\right) \right| dK_\chi dK_\psi \quad (10)$$

Equation (10) states that the peak aliasing current is bounded by an integral of the magnitude of the aliasing signal components in the passband. The evaluation of equation (10) is, however, not possible without having prior knowledge of the scene information distribution $\hat{O}(K_\chi, K_\psi)$; choices for $\hat{O}(K_\chi, K_\psi)$ must, therefore, be made which will yield useful bounds on any possible scene intensity distributions and, hence through equation (10), on the degree of aliasing degradation.

It is convenient to use an input spectrum which is constant in amplitude out to some cutoff frequency beyond the camera response. Hence, the reduction of aliasing is illustrated by comparing the results of performing the integration in equation (10) for $\hat{O}(K_\chi, K_\psi) = 1$.

PHOTOSENSOR APERTURE CONSIDERATIONS

The Concept of Aperture Shaping

Previous investigations concerned with the reduction of aliasing due to line-scan sampling (refs. 1 and 2) dealt with the intensity distribution of a scanning spot, either an electron beam in vidicon or orthicon tubes or a light beam in film facsimile reading and recording systems. Results from these investigations could be applied directly to the facsimile camera if the photosensor aperture could be shaded with a variable transmission. But this is generally not possible because of the very small dimensions involved, typically less than 1 millimeter across.

A procedure which is simpler to implement than aperture shading is aperture shaping; that is, the width of the photosensor aperture is adjusted to follow some curve which then adjusts the K_ψ spatial frequency characteristics of the aperture. To see that this is so, consider a general aperture function $P(\chi, \psi)$ which can be transformed to obtain spatial characteristics along azimuth ($K_\psi, K_\chi = 0$) where sampling, and hence aliasing, occurs. The function $P(\chi, \psi)$ is shaded to a definite spatial limit with a contour which is assumed expressible by one (or more) single valued function $f_n(\psi)$. This may be written

$$\begin{aligned}
\hat{P}(K_\psi, K_\chi=0) &= \int_{-\infty}^{\infty} \int_{-\infty}^{\infty} P(\chi', \psi') e^{-2\pi i K_\psi \psi'} d\chi' d\psi' \\
&= \int_{-\infty}^{\infty} \int_{f_1(\psi')}^{f_2(\psi')} P(\chi', \psi') e^{-2\pi i K_\psi \psi'} d\chi' d\psi' \\
&= \int_{-\infty}^{\infty} Q[\psi', f_2(\psi'), f_1(\psi')] e^{-2\pi i K_\psi \psi'} d\psi' \tag{11}
\end{aligned}$$

If a shaped aperture is now considered which has $P(\chi, \psi) = C$ and the width along χ is $W(\psi)$, then

$$\begin{aligned}
\hat{P}'(K_\psi, K_\chi=0) &= \int_{-\infty}^{\infty} \int_{-\infty}^{\infty} C e^{-2\pi i K_\psi \psi'} d\chi' d\psi' \\
&= \int_{-\infty}^{\infty} \int_{-\frac{W(\psi')}{2}}^{\frac{W(\psi')}{2}} C e^{-2\pi i K_\psi \psi'} d\chi' d\psi' \\
&= \int_{-\infty}^{\infty} W(\psi') C e^{-2\pi i K_\psi \psi'} d\psi' \tag{12}
\end{aligned}$$

Clearly, if $CW(\psi) = Q[\psi, f_2(\psi), f_1(\psi)]$, the following would result:

$$\hat{P}(K_\psi, K_\chi=0) = \hat{P}'(K_\psi, K_\chi=0) \tag{13}$$

Off the azimuth spatial frequency line $K_\chi = 0$, this equality no longer exists.

Realizability of Aperture Shapes

The realizability of aperture frequency response characteristics is based on the requirement that the aperture transmission always be greater than zero. This may be generalized by noting that any aperture transmission function, being always positive, must have a square root; that is, $P(\chi, \psi) = p^2(\chi, \psi)$, where $P(\chi, \psi)$ is the true aperture response and $p(\chi, \psi)$ is its square root. Taking the spatial transform and using the transform properties of the convolution yields

$$\mathcal{F}[P(\chi, \psi)] = \mathcal{F}[p^2(\chi, \psi)] = \int_{-\infty}^{\infty} \int_{-\infty}^{\infty} \hat{p}(K'_\chi, K'_\psi) \hat{p}(K_\chi - K'_\chi, K_\psi - K'_\psi) dK'_\chi dK'_\psi \tag{14}$$

In words, any realizable transfer function must, in the spatial frequency domain, be representable as the convolution of a function with itself. Given any response function, realiz-

able or not (it must, of course, be the transform of a real function), a fully realizable one can be generated simply by convolving it with itself. It should be noted that the aperture transmissions or shapes would be symmetric when generated in this fashion. However, it is symmetric apertures that are commonly of interest. Hence, for example, although the square modulation transfer function (MTF) resulting from a sinc function aperture is not realizable, a triangular MTF (the square MTF convolved with itself) resulting from a sinc² function aperture is realizable. Within this constraint, many MTF responses can be realized by aperture shaping.

Performance of Practical Aperture Shapes

A best aperture depends on the application of a specific system; and it involves a careful trade-off between MTF loss blurring, MTF cutoff, aliasing, and electronic noise. No practical aperture shape can, therefore, be considered as optimum in a general sense. But it can be demonstrated that aperture shapes other than the often used circular shape would generally be preferable. This is especially important when decrease in the azimuth sampling interval is limited by video data transmission constraints.

Analytical and experimental results are presented for three aperture shapes. The spatial outline and two-dimensional frequency response are shown in figure 4. The circular shape is presented as reference, and the diamond and cosine shapes are presented because they are superior to the circular shape in an interestingly different manner.

Analytical results.- Aliasing is numerically evaluated using equation (10). The object frequency distribution is assumed to be the least desirable case discussed previously; namely, $\hat{O}(K_\chi, K_\psi) = 1$. In addition, only the neighboring ($n = 1$) sideband is considered; all other contributors are small by comparison. The integral is taken over the bandpass region

$$-\frac{1}{2Y} < K_\chi < \frac{1}{2Y}$$

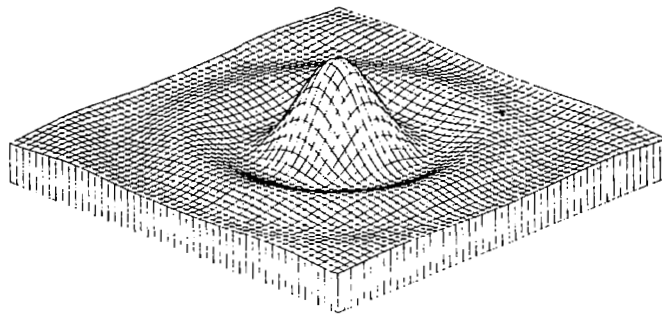
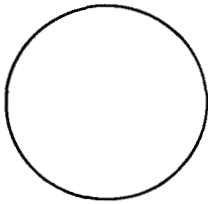
$$-\sqrt{\left(\frac{1}{2Y}\right)^2 - K_\chi^2} < K_\psi < \sqrt{\left(\frac{1}{2Y}\right)^2 - K_\chi^2}$$

which is a circle in the K_χ, K_ψ -plane. Results of the integration are presented in figure 5 as a function of the azimuth sampling interval. Also presented in this figure are two MTF sections of the aperture frequency response, one along the line-scan direction, the other along azimuth.

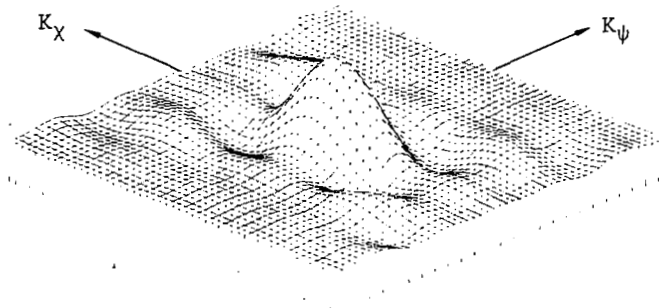
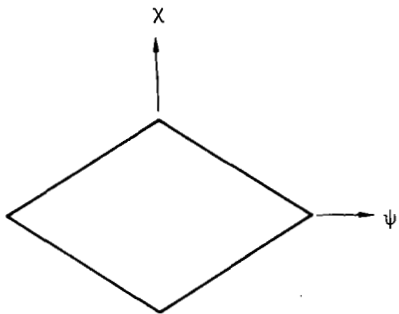
The MTF curves (figs. 5(a) and 5(b)) show little difference out to the normalized bandpass frequency of 0.5 ($1/2Y$). Spatial frequencies beyond this bandpass may be assumed to be eliminated by computer processing of the video data or significantly reduced by the image reproducer response. The main difference between the apertures

Spatial outline

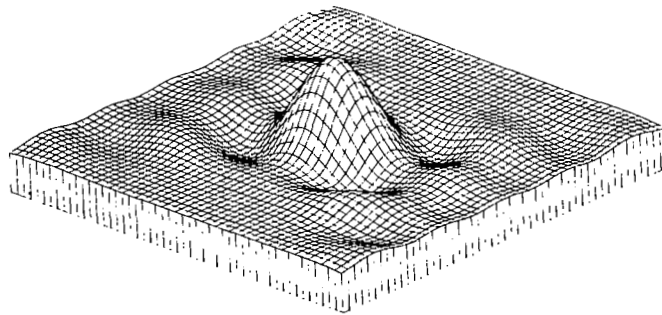
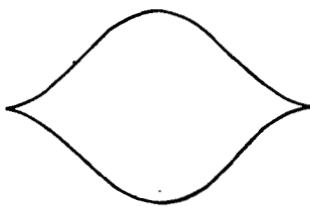
Frequency response



(a) Circle.

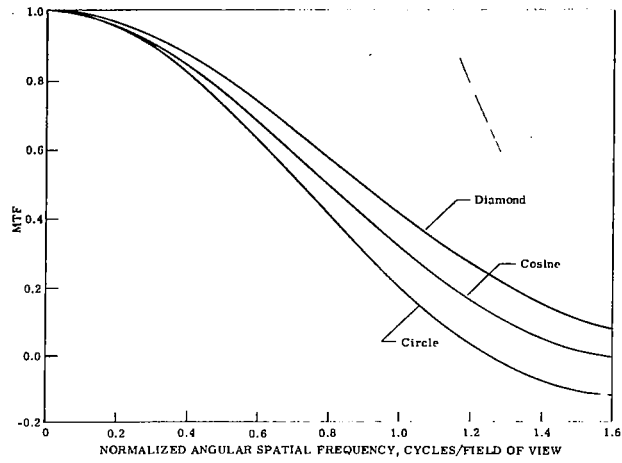


(b) Diamond.

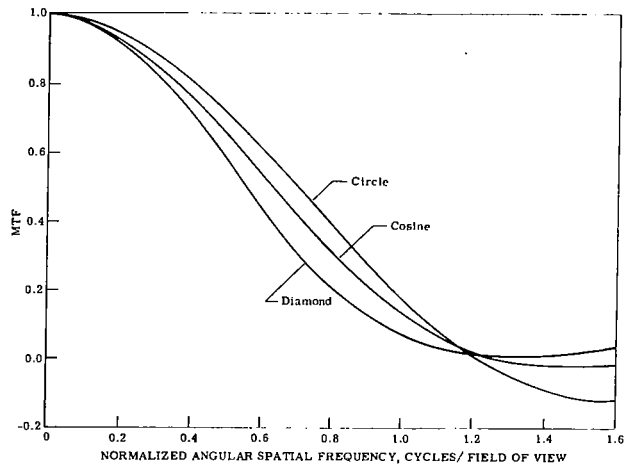


(c) Cosine

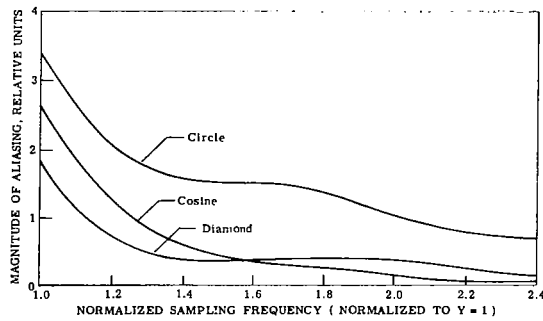
Figure 4.- Spatial outline and frequency response of three photosensor aperture shapes having equal area and equal width along the line-scan direction.



(a) Frequency response section along the line-scan direction.



(b) Frequency response section along azimuth direction.



(c) Variation of aliasing with line-scan spacing.

Figure 5.- Illustration of photosensor aperture shape characteristics.

is therefore the aliased signal within the reproduced bandpass. For the range of sampling intervals shown, both the diamond and the cosine aperture generate two to three times less aliasing than the circular aperture. It is interesting to note that the diamond shape generates less aliasing than the cosine shape for sampling rates less than 1.6 per instantaneous field of view or resolution element, whereas the cosine generates less aliasing for higher sampling rates.

Experimental results.- Figure 6 presents images obtained with the three photosensor apertures and different sampling rates. Several factors about these images may be



Circle

Diamond

(a) One line scan per instantaneous field of view.



Circle

Diamond

(b) 1.33 line scans per instantaneous field of view.



Circle

Cosine

(c) Two line scans per instantaneous field of view.

Figure 6.- Facsimile camera images resulting from use of different photosensor aperture shapes and line-scan spacings.

pointed out:

1. All images have essentially equal vertical resolution. This shows that the resolution of the camera frequency response along the line scan was not affected by the different photosensor aperture shapes. More important, the images show that the differences in image quality are caused by aliasing.

2. The most obvious extraneous patterns are significantly reduced when changing from the circular to the diamond aperture and a slightly increased sampling rate. But, a significant increase in effective resolution occurs also when changing from the diamond to the cosine aperture and a further increased sampling rate. This can be observed by carefully counting the number of lines (from left to right) and the number of rings (from the center) of the two targets, which can be unambiguously identified.

CONCLUDING REMARKS

The photosensor aperture of the facsimile camera, besides defining the instantaneous field of view, serves in many applications as the basic frequency bandlimiting filter of the entire system. Since the facsimile camera is a sampling system, this filter must be chosen with care. If the aperture limits the frequency response too much, contrast will be reduced by blurring; but if it limits too little, detail will be obscured by aliasing. A trade-off between these two image-degrading processes depends on specific applications and is generally difficult because aliasing is not only a function of the aperture shape but also of the scene information. But, as was shown, the amount of aliasing generated by circular photosensor apertures, which are most frequently used, can often be reduced two to three times by apertures of different geometrical shapes without significantly increasing blur.

Aliasing could be reduced without increasing blur by increasing the sampling rate (i.e., by decreasing the line-scan spacing). But this approach increases the amount of video data which must be transmitted, and a performance trade-off analysis must then include data transmission requirements. When this trade-off is made, it is important to recognize that apertures of different geometrical shapes are optimum in the rejection of aliasing for different line-scan spacings.

Langley Research Center,
National Aeronautics and Space Administration,
Hampton, Va., June 30, 1972.

REFERENCES

1. Mertz, P.; and Gray, F.: Theory of Scanning and Its Relation to Characteristics of Transmitted Signal in Telephotography and Television. Bell Syst. Tech. J., vol. 13, no. 3, July 1934, pp. 464-515.
2. Schade, Otto H.: Image Gradation, Graininess and Sharpness in Television and Motion-Picture Systems. Pt. III: The Grain Structure of Television Images. J. Soc. Motion Pict. & Telev. Eng., vol. 61, no. 2, Aug. 1953, pp. 97-164.
3. Selivanov, A. S.; Govorov, V. N.; Titov, A. S.; and Chemodanov, V. P.: Lunar Station Television Camera. Contract NAS 7-100, Reilly Translations, 1968. (Available as NASA CR-97884.)
4. Cherkasov, I. I.; Kemurdzhian, A. L.; et al.: First Panoramas of "LUNA-13" - Determination of Density and Mechanical Strength of Lunar Surface Layer at the Landing Site of the Automatic Station "LUNA-13." NASA CR-88874, 1967.
5. Brereton, R. G.; Burke, J. D.; Coryell, R. B.; and Jaffe, L. D.: Lunar Traverse Missions. JPL Quart. Tech. Rev., vol. 1, no. 1, Apr. 1971, pp. 125-137.
6. Mutch, T. A.; Binder, A. B.; et al.: Imaging Experiment: The Viking Lander. Int. J. Solar Syst. Stud., vol. 16, no. 1, Feb. 1972, pp. 92-110.
7. Goodman, Joseph W.: Introduction to Fourier Optics. McGraw-Hill Book Co., c.1968.
8. Carlson, A. Bruce: Communications Systems. McGraw-Hill Book Co., c.1968.
9. Huck, Friedrich O.; and Lambiotte, Jules J., Jr.: A Performance Analysis of the Optical-Mechanical Scanner as an Imaging System for Planetary Landers. NASA TN D-5552, 1969.